Novel Substrate Integrated Waveguide Architectures for Microfluidic Biosensing and Environmental Detection

Adel Benleulmi, Naimi Boubekeur, and Daniel Massicotte
Department of Electrical and Computer Engineering, Université du Québec à Trois-Rivières
Trois-Rivières, QC G8Z 4M3, Canada.
adel.benleulmi@uqtr.ca

***Abstract*— This paper presents two novel substrate integrated waveguide (SIW) sensing-elements for microfluidic biosensing and environmental detection. The first proposed structure is a SIW interferometer for biological liquids characterization. The operation principle of the latter is based on the variation of the effective dielectric constant of a sensitive branch due to the introduction of aqueous solutions into a sensitive region of a total volume of ~1 µL. To achieve a destructive interference, the signal division and combination have been carried out using microstrip Wilkinson power dividers. The sensitive characteristics of the device have been tested by measuring two buffer solutions; Phosphate-buffered saline (PBS) and Roswell Park Memorial Institute medium (RPMI). In regards to the second proposed device, it consists of an H-plane SIW-based horn antenna demonstrated for relative humidity (RH) sensing. The sensitive characteristics of the proposed antenna without the use of a sensitive layer were tested in the range of 25%–75% RH. The combination of antenna and sensor functions in a single substrate integrated device offers multiple advantages and enables the development of simple, compact and cost-effective sensors. Passive RFID sensing is also possible with this technique without resorting to the use of additional sensors.**

Keywords—Interferometer, Horn antenna, Sensor, Biological liquids, Humidity, Substrate Integrated Waveguide (SIW).

I. Introduction

Various architectures of SIW sensors have been demonstrated and presented in literature for dielectric materials' characterization as for environmental detection [1]–[4].

Biosensing, as one of the most relevant functions in materials' characterization, is crucial within the vast majority of healthcare applications. In fact, the use of biosensors provides physicians and experts with highly valuable information that helps them diagnose patients, prevent diseases and even discover new drugs [5]–[6]. Various types of biosensors based on distinct technologies were presented in literature. For instance, an optical interferometric sensor for biological and chemical sensing was investigated in [7]. In [8], a 3 µL biosensor based on a SIW cavity resonator was demonstrated. The sensing behavior of the latter was tested with fibroblast cells from the lungs of a human male subject.

In environmental detection, humidity presents one of the important parameters that should be monitored to insure a good air quality in houses, medical institutions and even to preserve the quality of stored food [9]–[10]. For this reason, many microwave sensing-components and techniques have been investigated and presented in literature. For instance, a humidity sensor based on a chipless RFID tag structure integrating a U shaped slot loaded rectangular tag with an ELC resonator was demonstrated in [11]. A polyvinyl-alcohol (PVA) film was used as a humidity sensitive layer. In [3], humidity sensing with SIWs has been demonstrated for the first time with a cavity resonator in which the operation frequency varied depending on the RH level. The presented structure exhibited satisfactory sensing capabilities without the use of a sensitive material. Recently, a new generation of radio frequency (RF) interferometers based on SIW technology was demonstrated in [12]; the presented structure was studied as a humidity sensing-element to exhibit its potential for sensing applications.

In this study, two new architectures of SIW sensing-elements are introduced. The first device, a SIW interferometer, is proposed for characterization purposes; for a 33% lower operation frequency, its overall size was reduced by ~45% -compared to the previous architecture- and its effective quality factor was significantly enhanced. The Wilkinson power dividers, considered for the signal division and combination, ensure the good functioning of the device over a large operation frequency range.

In regards to the second device, an SIW-based H-plane horn antenna is demonstrated for humidity sensing. The proposed structure was designed, manufactured and validated experimentally. The antenna was functionalized using a sensitive region composed of an air holes array. No humidity-sensing material was used. Measurements at different relative humidity levels from 25%–75% RH were performed. The proposed structure could be adjusted for a desired operation frequency and sensitive layers could be applied for sensitivity enhancement or even the detection of other physical quantities such as gas or temperature.

II. SIW Microfluidic Interferometric Biosensor

A. Interferometer design and operation

The SIW interferometric biosensor was designed using the 3D electromagnetic software High Frequency Structural Simulator (HFSS) and co-simulated with Advanced Design System (ADS). The considered dimensions of the structure are: W_{adpt} = 3.7 mm, W_0 = 1.2 mm, W_t = 6.3 mm, W_{S1} = 12.66 mm, W_{S2} = 14.66 mm, L_m = 5 mm, L_t = 2.5 mm, D_{diel} = 0.9 mm, $D_{metalized}$ = 0.6 mm, $b_{metalized}$ = 1 mm, l_1 = 15.59 mm, l_2 = 5.59 mm. The used substrate is Rogers 4003C (ε_r= 3.55, tan δ = 0.0023, h = 1.524 mm). Fig. 1 shows the architecture of the substrate integrated interferometer.

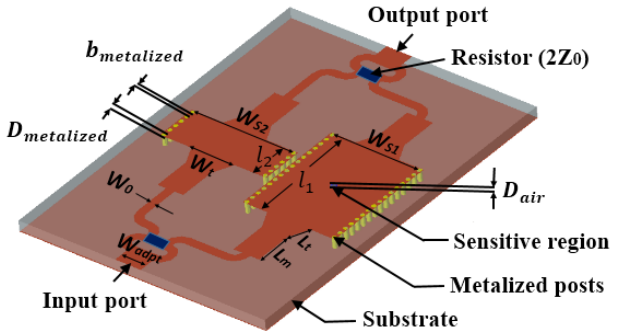

(a)

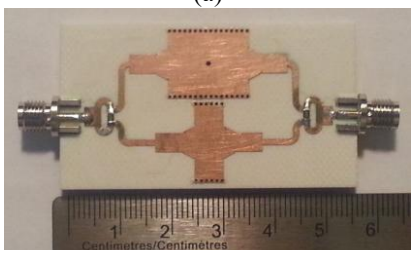

(b)

Fig. 1. Architecture of the SIW interferometric biosensor: (a) Design parameters of the SIW interferometer, (b) Manufactured circuit.

The phase difference between the structure's branches at a frequency f is given by

(1)

where β_1 and β_2 are the phase constants of the sensitive branch and the reference branch, respectively.

Since the two branches are designed for a signal destructive interference at the output port (i.e., a phase difference of 180°), equation (1) can be written for TE_{10} mode as

(2)

where denotes the speed of electromagnetic waves in vacuum, is the operation frequency, and $W_{eff1,2}$ is the effective width of each branch. The effective dielectric constant of the sensitive branch changes depending on the tested sample's permittivity ε_r(MUT) and its variation can be estimated by the Maxwell-Garnett (MG) mixing rule [2]

(3)

where v is the volume fraction of the sensitive region. Therefore, the introduction of the biomaterial under test changes the effective permittivity of the sensitive branch, which causes the operation frequency shift.

B. *Experimental validation*

A comparison between the measured and simulated S_{21} modulus of the device after optimization is shown in Fig. 2. The obtained results are in good accordance and the difference between the simulation and measurement is mainly due to the circuit imperfections and simulations error. The corresponding measured effective quality factor, defined as $Q_{eff} = f_0/\Delta f_{3dB}$, is 1.1×10^4.

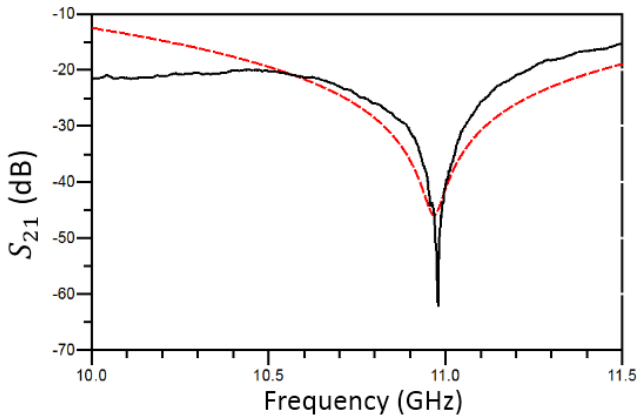

Fig. 2. Simulated and measured S_{21} modulus of the device.

The sensitive characteristics of the device have been tested by measuring two aqueous solutions commonly used in cell culture applications; Phosphate-buffered saline (PBS) and Roswell Park Memorial Institute medium (RPMI). The aim of measuring these liquids is to investigate the proposed structure's potential in applications relating to cellular biology such as cell counting and comparison.

The samples were injected into the sensitive region using an automatic pipette set to 1 µL. The injected volumes held perfectly in the dielectric hole by capillary action. No layers were used to prevent the liquids from leaking. Once the measurements taken, the samples under test were retrieved from the device by using the same micropipette. A new sterile conical tip was used in each manipulation. Fig. 3 displays the measurement setup together with the used automatic pipette.

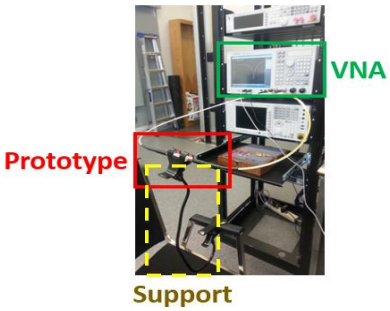

(a)

(b)

Fig. 3. Photograph of the measurement configuration: (a) Measurement setup, (b) Used micropipette.

Fig. 4 shows the measurement results of the proposed interferometer. The S_{21} modulus of the device was first measured in the absence of the buffer solutions; these latter were introduced afterwards in the sensitive branch and measured separately. Finally, measurements after retrieving the samples were taken.

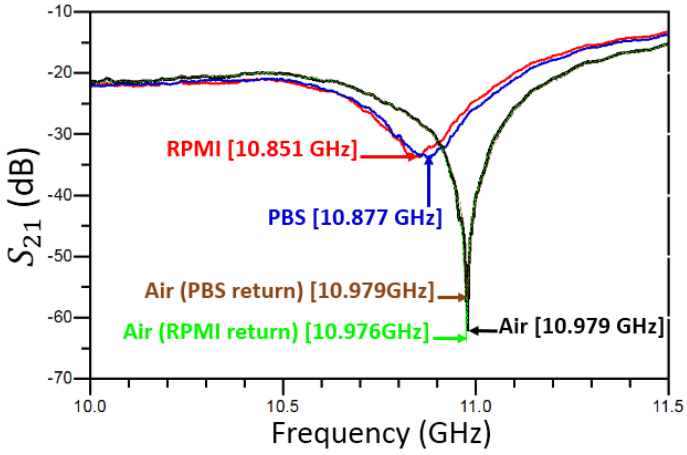

Fig. 4. Measured S_{21} modulus of the buffer solutions.

According to Fig. 4, the presence of buffer solutions in the sensitive region caused a significant shift of the operation frequency while maintaining a good visibility of the latter. In fact, the measured level of the S_{21} modulus in both cases is less than -30 dB and the frequency shifts are $\Delta f_{(PBS)}$= 102 MHz and $\Delta f_{(RPMI)}$= 128 MHz. The operation frequency is easily detectable especially with the total absence of any parasitic frequencies. Also, based on its return to the initial state with a frequency shift less than 3 MHz (RPMI return), the effect of the absorption/adsorption phenomena is ascertained to be small if existing. Hence, this possibility of retrieving the biomaterial under test after measurement presents a major advantage of the proposed device; this is important especially in cases where the available volumes are limited and there is a wide range of tests to be performed. In those cases, the wastage or destruction of samples is not tolerable.

As a next step, the proposed device can be considered in the detection of different cell concentrations to determine the lowest detectable concentration and subsequently consider it in future experiments. In presence of cells, the effective permittivity of the buffer solutions decreases. Therefore, the operation frequency is expected to shift to the right for higher cell concentrations.

III. H-Plane Substrate Integrated Waveguide Horn Antenna for Humidity Sensing

A. Antenna sensor design & operation principle

The SIW antenna sensor was designed and simulated using HFSS. The design technique of SIW H-plane horn antennas presented in [13], [14] was taken into account while conceiving the sensor. To improve the performance of the proposed SIW antenna, a printed transition which consists of a two block parallel plate waveguides was etched after the horn aperture. This transition has a length L_i and separation gaps of a width S_i. The considered dimensions of the structure are presented in Table I. The used substrate is Rogers 4003C (εr= 3.55, tan δ = 0.0023, h = 1.524 mm). Fig. 5 shows the architecture of the SIW antenna sensor. The structure of the antenna with all the parameters is shown in Fig. 5a while the manufactured circuit is shown in Fig. 5b.

TABLE I
DESIGN PARAMETERS VALUES FOR THE SIW HORN ANTENNA (UNIT: MILLIMETER)

W_{adpt}	L_t	t	S	W_1	W_2	D_1	D_2
3.38	4.5	2.21	0.735	11	26.4	28.8	22.8

D_{air}	b_{air}	$D_{metalized}$	$b_{metalized}$	S_0	S_1	L_1	L_2
1	1.7	1.1	2	0.4	0.9	4	4

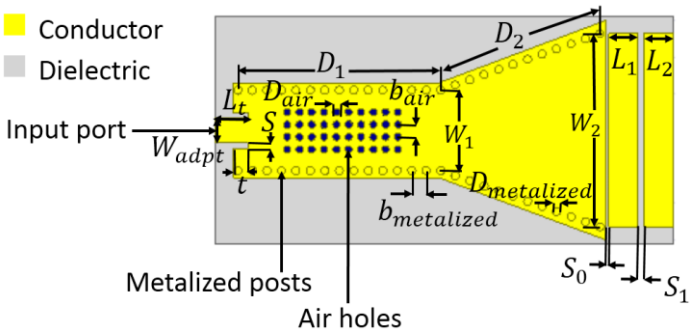

(a)

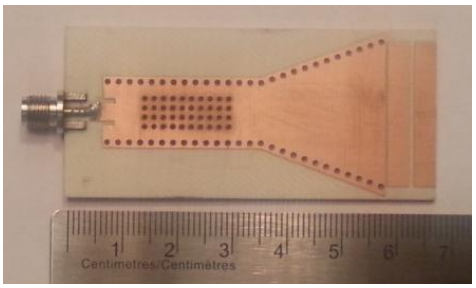

(b)

Fig. 5. Architecture of the SIW antenna sensor: (a) Design parameters of the SIW antenna, (b) Manufactured circuit.

The sensor's operation principle is based on the variation of the dielectric constant of moist air in function of the relative humidity percentage as given by [15]

— — (4)

where is the absolute temperature (K), is the pressure of moist air (mmHg), is the pressure of saturated water vapor (mmHg), and is the relative humidity (%). The variation of moist air's relative permittivity inside the air holes array leads to a change in the effective permittivity of the structure as estimated by the Maxwell-Garnett mixing rule [2]

$$\varepsilon_{eff} = \varepsilon_r + 3v\varepsilon_r \frac{\varepsilon_r(H)-\varepsilon_r}{\varepsilon_r(H)+2\varepsilon_r-v(\varepsilon_r(H)-\varepsilon_r)} \quad (5)$$

Therefore, it affects the operation frequency which shifts depending on the relative humidity percentage.

B. Experimental validation of humidity sensing

A comparison between the simulated and measured S_{11} modulus of the device after optimization at 25% RH and 30 °C is shown in Fig. 6. The simulation result is in accordance with the measured S_{11}. The difference is due to the fabrication imperfections.

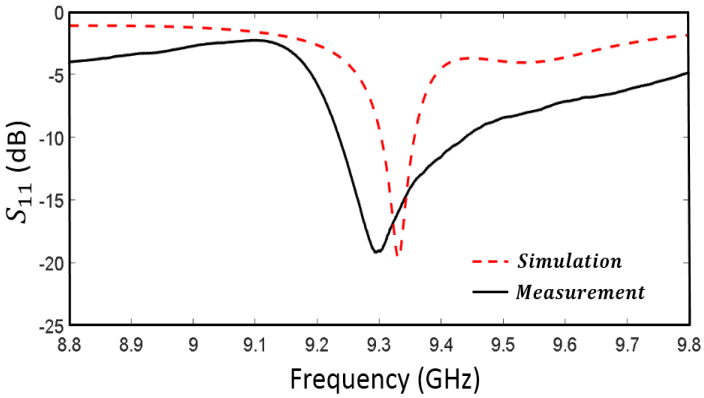

Fig. 6. Simulated and measured S_{11} modulus at 25% RH.

The sensitive characteristics of the proposed antenna were tested experimentally for T around 30 °C in the range of 25%–75% RH using the experimental setup presented in Fig. 7.

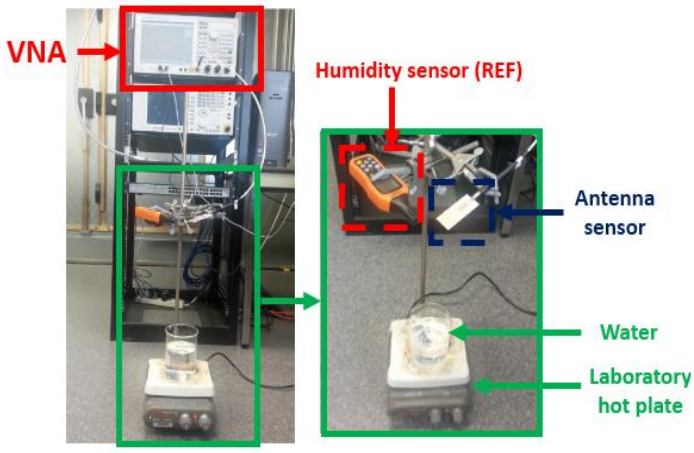

Fig. 7. Photograph of the measurement setup.

The tests were carried out within this humidity range to avoid the accumulation of water molecules in the air holes array at higher relative humidity percentages. In fact, water condensation would cause a significant frequency shift due to the important change in the effective dielectric constant of the SIW antenna. The experiments were conducted in a closed room with a temperature of 21.5°C and a relative humidity of ~25% RH. The control of the relative humidity level at which the device was exposed was carried out by gradually increasing the temperature of the laboratory hot plate and taking measurements with the reference sensor. A stabilization time of around 15 minutes was kept for each RH% step. Fig. 8 shows the measured S_{11} modulus at 25% and 75% RH in the frequency range of 8.8 GHz to 9.8 GHz.

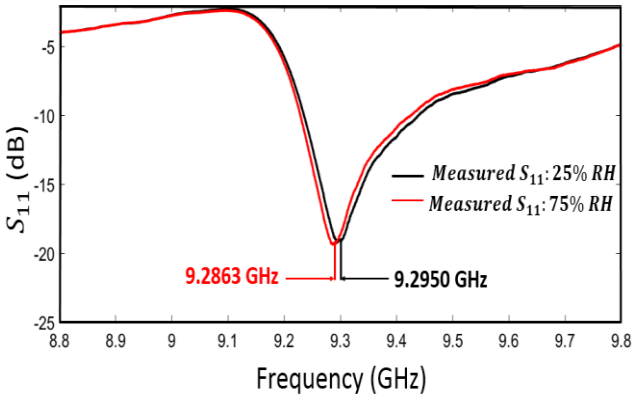

Fig. 8. Measured S_{11} modulus at 25% and 75% RH.

Fig.8. revealed the structure to be sensitive to the variation of the relative humidity percentage as the antenna's operation frequency shifted by 8.7 MHz. The experiment was repeated three times under the same experimental conditions to test the measurements repeatability. Due to the instability of the measurement setup and the reference sensor errors, the estimated RH measurement uncertainty was around 8 % RH. Fig. 9 shows the measurement results at different relative humidity levels. As shown in this figure, the structure exhibited a sensitivity of 174 kHz/RH from 25% to 75% RH. The antenna sensor was measured in an anechoic chamber and the measurement results of the H- and E- plane radiation patterns at 9.29 GHz, 9.28 GHz and 9.27 GHz are shown in Fig. 10.

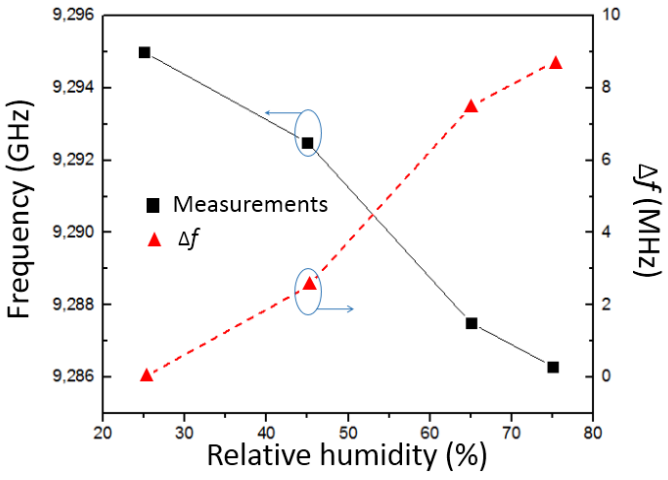

Fig. 9. Sensitivity characteristics of the SIW horn antenna: (Left axis) the measured operation frequency as a function of the relative humidity variation. (Right axis) operation frequency variation.

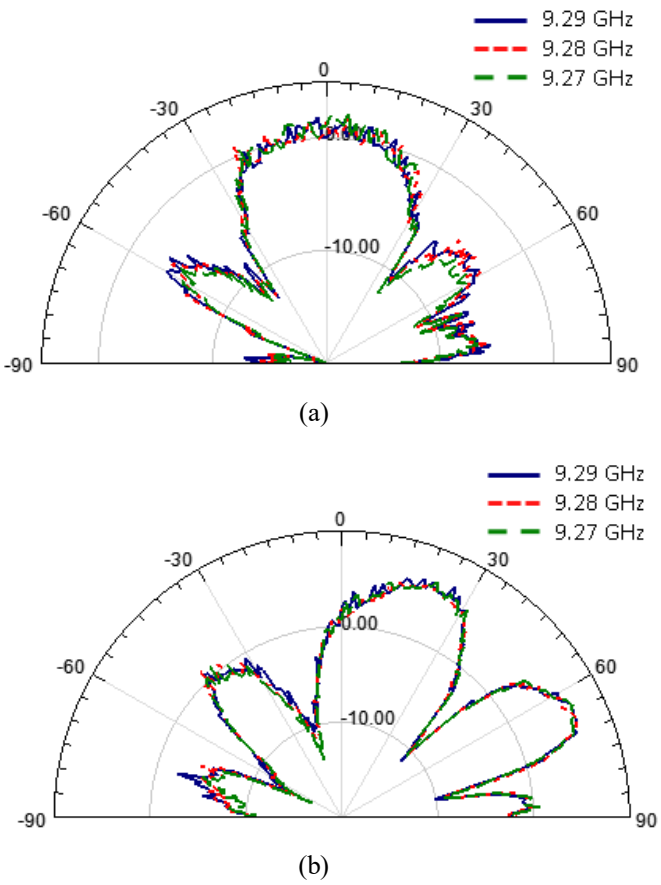

Fig.10. Measured radiation pattern [dBi] of the antenna sensor: (a) H-plane, (b) E-plane.

IV. Conclusion

In this paper, two architectures of SIW sensing-elements are introduced. First, a microfluidic substrate integrated interferometer for biological liquids characterization has been presented. The proposed interferometer has been tested by measuring two aqueous solutions commonly used in cell culture applications (PBS and RPMI). The developed structure presents a good effective quality factor (Q_{eff}=1.1×10^4) with a S_{21} modulus less than -60 dB at the operation frequency of 10.98 GHz. The required total volume is only 1 µL with possibility of retrieving the sample after measurements. In regards to the second device, a novel antenna sensor based on SIW technology has been presented. The proposed H-plane horn antenna has been demonstrated for relative humidity sensing without the use of a sensitive material and exhibited a sensitivity of 174 kHz/RH in the range of 25%–75% RH. This sensitivity could be significantly enhanced by using an appropriate sensitive material. The latter could be chosen for the detection of physical quantities other than humidity. The advantages of the proposed structures in terms of compactness and cost-efficiency in addition to their passive operation make them an interesting solution for biosensing and environmental detection.

References

[1] M. Bozzi, A. Georgiadis, and K. Wu, "Review of substrate integrated waveguide circuits and antennas," *IET Microw. Antennas Propag.*, vol 5, no. 8, pp. 909–920, Jun. 2011.

[2] J. D. Barrera and G. H. Huff, "Analysis of a variable SIW resonator enabled by dielectric material perturbations and applications," *IEEE Trans. Microw. Theory Techn.,* vol. 61, no. 1, pp. 225–233, Jan. 2013.

[3] H. El Matbouly, N. Boubekeur, and F. Domingue, "Passive Microwave Substrate Integrated Cavity Resonator for Humidity Sensing," *IEEE Trans. Microw. Theory Techn.*, vol.63, no.12, pp.4150-4156, Dec. 2015.

[4] A. Benleulmi, N. Y. Sama, P. Ferrari, and F. Domingue, "Substrate Integrated Waveguide Phase Shifter for Hydrogen Sensing," *IEEE Microw. and Wireless Compon. Lett.*, vol. 26, no. 9, pp. 744-746, Sept. 2016.

[5] D.R. Thevenot, K. Toth, R.A. Durst, and G.S. Wilson, "Electrochemical biosensors: recommended definitions and classification", *Pure Appl. Chem*., vol 71, no. 12, pp. 2333–2348, 1999.

[6] D.R. Thevenot, K. Toth, R.A. Durst, and G.S. Wilson, "Electrochemical biosensors: recommended definitions and classification", *Biosens. Bioelectron.*, vol. 16, no. (1–2), pp. 121–131, 2001.

[7] K. Kim and T.E. Murphy, "Porous silicon integrated Mach-Zehnder interferometer waveguide for biological and chemical sensing", *Opt. Express*, vol 21, no. 17, pp. 19488–19497, 2013.

[8] A. Salim, S. Kim, J.Y. Park, and S. Lim, "Microfluidic Biosensor Based on Microwave Substrate Integrated Waveguide Cavity Resonator," *J. Sens*., vol. 2018, Article ID 1324145, 13 pages, 2018.

[9] G. Marrocco, "Pervasive electromagnetics: sensing paradigms by passive RFID technology," *IEEE Wireless Commun.*, vol. 17, no. 6, pp. 10 –17, Dec. 2010.

[10] S. Manzari, C. Occhiuzzi, S. Nawale, A. Catini, C. Di Natale, and G. Marrocco,"Humidity Sensing by Polymer-Loaded UHF RFID Antennas," *IEEE Sensors J.*, vol. 12, no. 9, pp. 2851-2858, Sept 2012.

[11] E. M. Amin, M. S. Bhuiyan, N. C. Karmakar, and B. Winther-Jensen, "Development of a Low Cost Printable Chipless RFID Humidity Sensor," *IEEE Sensors J.*, vol. 14, no. 1, pp. 140-149, Jan. 2014.

[12] A. Benleulmi, N. Boubekeur, and D. Massicotte, "A Highly Sensitive Substrate Integrated Waveguide Interferometer Applied to Humidity Sensing," *IEEE Microw. and Wireless Compon. Lett.*, vol. 29, no. 1, pp. 68-70, Jan. 2019.

[13] M. Esquius-Morote, B. Fuchs, J. Zürcher, and J. R. Mosig, "A Printed Transition for Matching Improvement of SIW Horn Antennas," *IEEE Trans. Antennas Propag.*, vol. 61, no. 4, pp. 1923-1930, Apr 2013.

[14] M. Esquius-Morote, B. Fuchs, J. Zürcher, and J. R. Mosig, "Novel Thin and Compact H-Plane SIW Horn Antenna," *IEEE Trans. Antennas Propag.*, vol. 61, no. 6, pp. 2911-2920, Jun. 2013.

[15] J. Fraden, The Handbook of Modern Sensors: Physics, Design and Application, 3rd ed. New York, NY, USA: Springer, 2003, pp. 393–399.